Contents

Experimental Section

General:

^{1}H and ^{13}C NMR spectra were recorded with a JEOL JNM ECZ-500R instrument at 500 and 125 MHz. Mass spectra were obtained with a Bruker microTOF II spectrometer. UV/visible absorption spectra were acquired using a JASCO V-730 spectrometer. Emission spectra were obtained using a Jasco FP-8500 spectrometer. Quantum yields were measured by the absolute method using a Jasco FP-8500 spectrometer equipped with a Jasco ILF-835 integrating sphere. Temperature dependent emission spectra were obtained using a Jasco FP-6500 spectrometer. Quantum yields at 77 K were measured by the absolute method using a Jasco FP-6500 spectrometer equipped with a Jasco INK-533 integrating sphere. Time dependent emission decay was measured on a Hamamatsu Photonics Quantaurus-Tau fluorescence lifetime system. Circular dichroism (CD) spectra were recorded on a JASCO J-1500 spectropolarimeter at room temperature; two scans were accumulated. Circularly polarized luminescence (CPL) spectra were recorded on a JASCO CPL-300 at room temperature. Spin-coated film was fabricated with a MIKASA MS-B100 spin-coater. All samples for CPL were excited around 350 nm. In the meaurement on CPL, eight scans for toluene solution and six scans for spin-coated PMMA film were accumulated.

Synthesis

Synthesis of (R_p, R_p)-**2**

A mixture of (R_p)-**1** (118.5 mg, 0.37 mmol), Pt(dtbpy)Cl_2 (211.4 mg, 0.38 mmol), CuI (14.7 mg 0.077 mmol) was placed in a round-bottom flask equipped with a magnetic stirring bar. After degassing the reaction mixture several times, degassed solutions of CH_2Cl_2 (60 mL) and Et_3N (30 mL) were added to the mixture. After the mixture was stirred at room temperature for 5 days, H_2O and CH_2Cl_2 was added to the reaction mixture. The organic layer was extracted with CH_2Cl_2 and washed with brine. The organic layer was dried over $MgSO_4$ and then $MgSO_4$ was removed by filtration. After the solvent was removed with a rotary evaporator, the residue was purified by column chromatography on NH-SiO_2 (CH_2Cl_2/MeOH = 20/1 v/v as eluent). Further purification was carried out by gel permeation chromatography (CH_2Cl_2) to afford (R_p, R_p)-**2** (87.9 mg, 0.057 mmol, 31%) as a dark red solid.

R_f = 0.93 (CH_2Cl_2/MeOH = 20/1 v/v). ^{1}H NMR ($CDCl_3$, 500 MHz) δ 1.41 (s, 36H), 2.77 (m, 4H), 3.14 (m, 8H), 3.68 (s, 12H), 3.71(m, 4H), 6.08 (s, 4H), 7.44 (dd, J = 1.7, 5.7 Hz, 4H), 7.52 (s, 4H), 7.87 (d, J = 1.7 Hz, 4H), 9.85 (d, J = 5.7 Hz, 4H) ppm; ^{13}C NMR ($CDCl_3$, 125 MHz) δ 29.1, 30.3, 33.6, 35.7, 55.2, 85.6, 102.3, 113.4, 118.3, 122.6, 124.0, 126.1, 137.6, 144.0, 151.8, 156.2, 156.6, 162.6 ppm. IR(ATR): $\tilde{\nu}$ = 2962, 2930, 2098, 1484, 1415, 1248, 1205, 1091, 846, 713 cm^{-1}. HRMS (ESI) calcd. For $C_{80}H_{85}N_4O_4Pt_2$ $[M+H]^+$: 1555.5866, found for 1555.5861.

(S_p, S_p)-**2** was obtained in 22% yield by the same procedure of (R_p, R_p)-**2**.

Synthesis of **3**

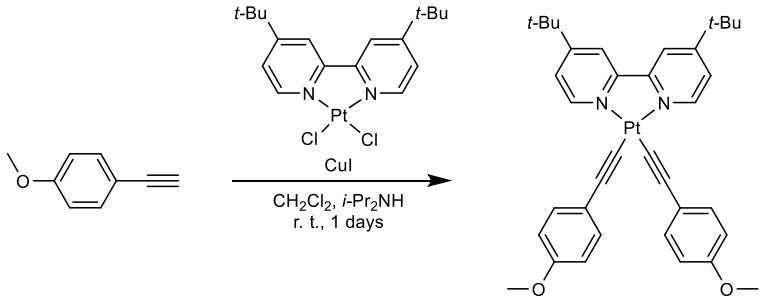

3
75%

A mixture of 4-ethynylanisole (185.0 mg, 1.4 mmol), Pt(dtbpy)Cl_2 (106.8 mg, 0.2 mmol), CuI (20.0 mg 0.1 mmol) was placed in a round-bottom flask equipped with a magnetic stirring bar. After degassing the reaction mixture several times, degassed solutions of CH_2Cl_2 (80 mL) and diisopropylamine (20 mL) were added to the mixture. After the mixture was stirred at room temperature for 1 days, the solvent was removed with a rotary evaporator. The residue was purified by recrystallization (CH_2Cl_2/Hexane) to afford **3** (111.1 mg, 0.15 mmol, 75%) as an orange solid.

^{1}H NMR ($CDCl_3$, 500 MHz) δ 1.44 (s, 18H), δ 3.80 (s, 6H), 6.80 (d, J = 8.6 Hz, 4H), δ 7.51 (br, 2H), 7.56 (dd, J = 2.3, 6.3 Hz, 2H), δ 7.95 (d, J = 1.2 Hz, 2H), 9.71 (br, 2H) ppm; ^{13}C NMR ($CDCl_3$, 125 MHz) δ 30.25, 35.80, 55.24, 113.24, 118.90 (two peaks), 124.59, 133.38, 150.94 (two peaks), 156.20, 157.66, 163.35 ppm. IR(ATR): $\tilde{\nu}$ = 2964, 2902, 2833, 2133, 1504, ,1417, 1238, 1030, 827 cm^{-1}. HRMS (ESI) calcd. For $C_{36}H_{38}N_2O_2PtNa$ $[M+Na]^+$: 748.2476, found for 748.2481.

X-ray structure determination: Crystals suitable for X-ray diffraction studies were analyzed using a Rigaku MicroMax-007HFM MoKa rotating anode generator equipped with VariMax optics, an AFC1 goniometer, and Saturn 724+ detector. The reflection data for them was integrated, scaled and averaged using Rigaku CrysAlis^{PRO}. The structures were solved by a direct method (SHELXT) and refined using a full-matrix least-squares method on F2 for all reflections (SHELXL-2018/3). The solvent molecules were "squeezed" during the structure refinement. All calculations were performed on the Olex2 program package. Crystallographic data are given in Table S1 in the Supporting Information. CCDC-2022660 ((R_p, R_p)-**2**) contain the supplementary crystallographic data for this paper. These data can be obtained free of charge from The Cambridge Crystallographic Data Centre via https://www.ccdc.cam.ac.uk/structures/

Computational methods

DFT calculations were carried out by using the Gaussian 16 program package,[1] with the LanL2DZ basis set for Pt atoms and 6-31G(d) for C, H, N, and O atoms. Optimized geometries in the ground and triplet states were determined by DFT calculations with the MN15 functional, which shows excellent performance in the calculation of structures, energies, and properties of organic and inorganic molecules. TD-DFT and SOC-TD-DFT calculations were carried out by using Orca program package,[2] with the SARC-ZORA-SVP basis set for Pt atoms and ZORA-SVP basis set for C, H, N, and O atoms with ZORA Hamiltonian. The energy levels, electronic configurations, CPL parameters in the single and SOC excited states were estimated from TD-DFT and SOC-TD-DFT calculations, respectively, with LC-BLYP functional.

[1] Gaussian 16, Revision B.01, M. J. Frisch, G. W. Trucks, H. B. Schlegel, G. E. Scuseria, M. A. Robb, J. R. Cheeseman, G. Scalmani, V. Barone, G. A. Petersson, H. Nakatsuji, X. Li, M. Caricato, A. V. Marenich, J. Bloino, B. G. Janesko, R. Gomperts, B. Mennucci, H. P. Hratchian, J. V. Ortiz, A. F. Izmaylov, J. L. Sonnenberg, D. Williams-Young, F. Ding, F. Lipparini, F. Egidi, J. Goings, B. Peng, A. Petrone, T. Henderson, D. Ranasinghe, V. G. Zakrzewski, J. Gao, N. Rega, G. Zheng, W. Liang, M. Hada, M. Ehara, K. Toyota, R. Fukuda, J. Hasegawa, M. Ishida, T. Nakajima, Y. Honda, O. Kitao, H. Nakai, T. Vreven, K. Throssell, J. A. Montgomery, Jr., J. E. Peralta, F. Ogliaro, M. J. Bearpark, J. J. Heyd, E. N. Brothers, K. N. Kudin, V. N. Staroverov, T. A. Keith, R. Kobayashi, J. Normand, K. Raghavachari, A. P. Rendell, J. C. Burant, S. S. Iyengar, J. Tomasi, M. Cossi, J. M. Millam, M. Klene, C. Adamo, R. Cammi, J. W. Ochterski, R. L. Martin, K. Morokuma, O. Farkas, J. B. Foresman, and D. J. Fox, Gaussian, Inc., Wallingford CT, 2016.

[2] F. Neese, F. Wennmohs, U. Becker, C. Riplinger. The ORCA quantum chemistry program package. *J. Chem. Phys.* **2020,** *152*, 224108–224118.

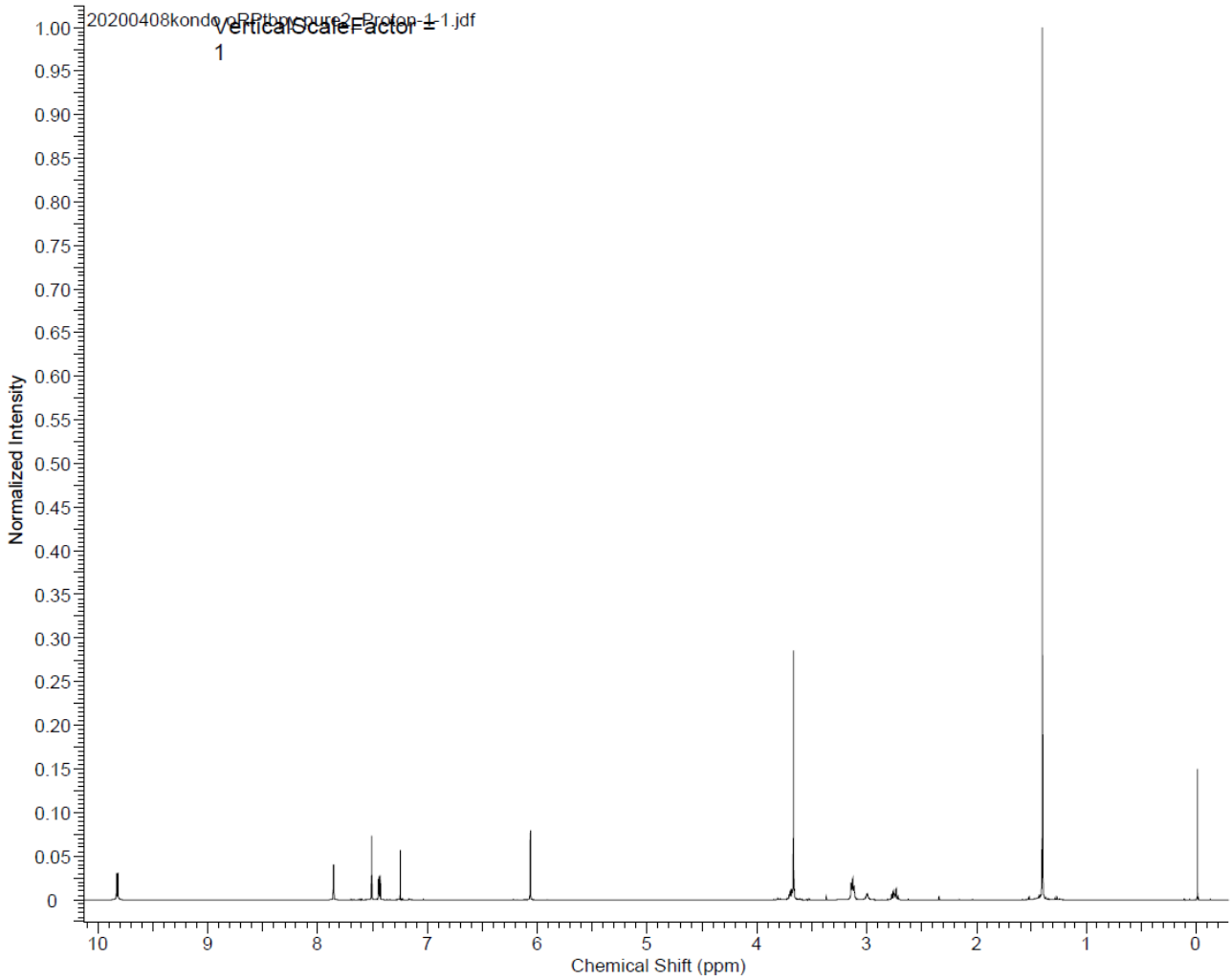

Fig. S1 ^{1}H NMR spectrum of (R_p,R_p)-**2** ($CDCl_3$, 500 MHz).

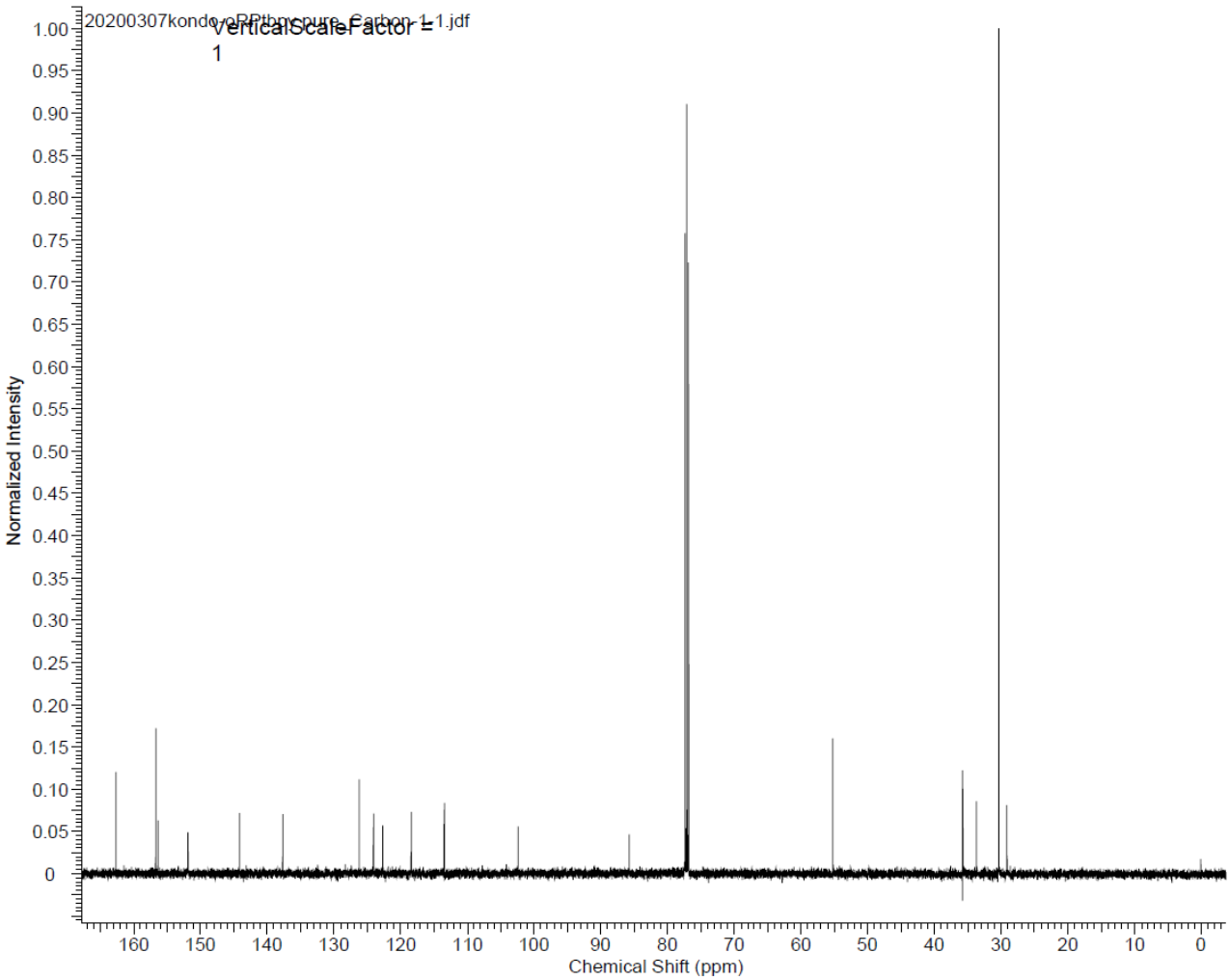

Fig. S2 ^{13}C NMR spectrum of (R_p,R_p)-**2** ($CDCl_3$, 125 MHz).

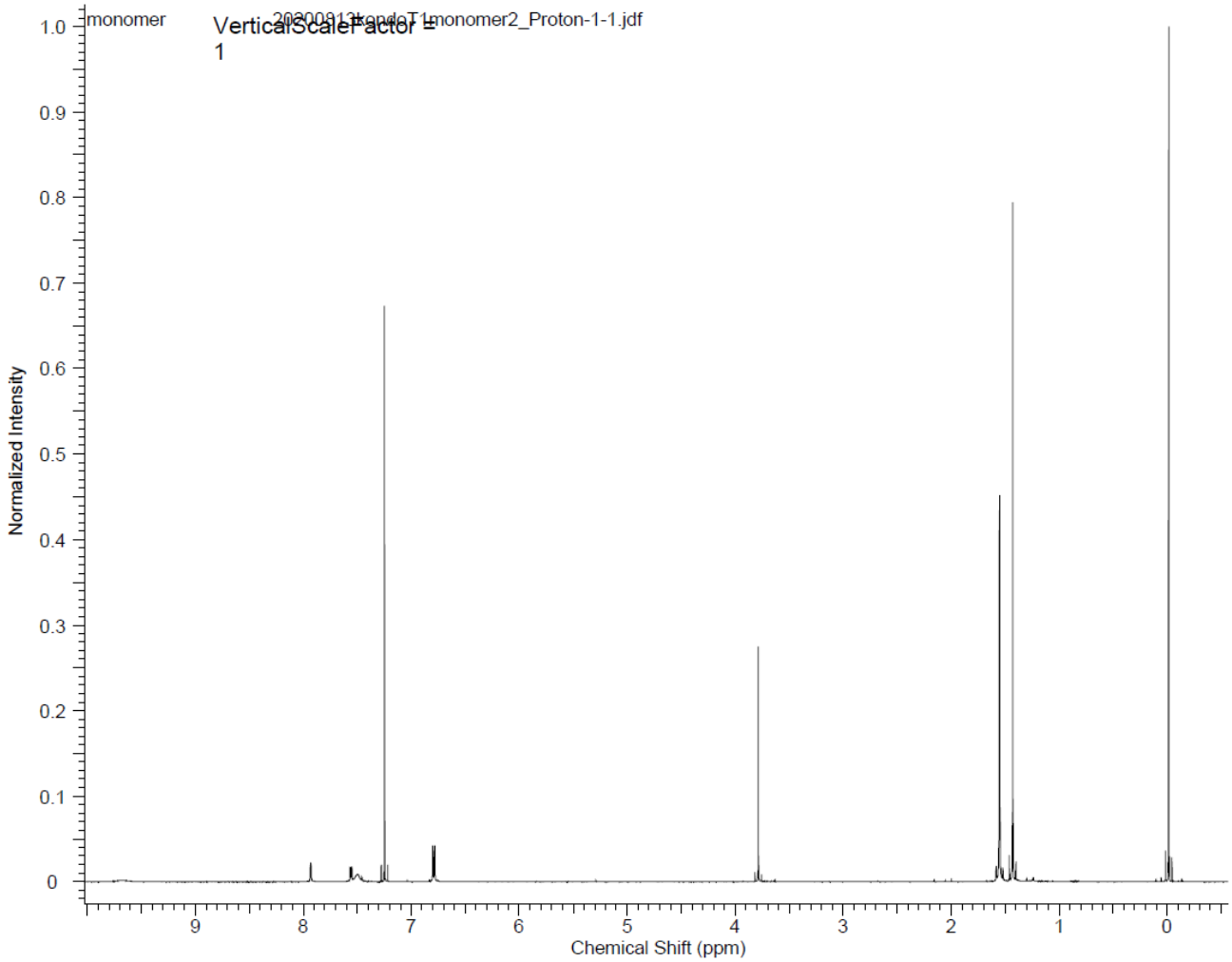

Fig. S3 ^{1}H NMR spectrum of **3** ($CDCl_3$, 500 MHz).

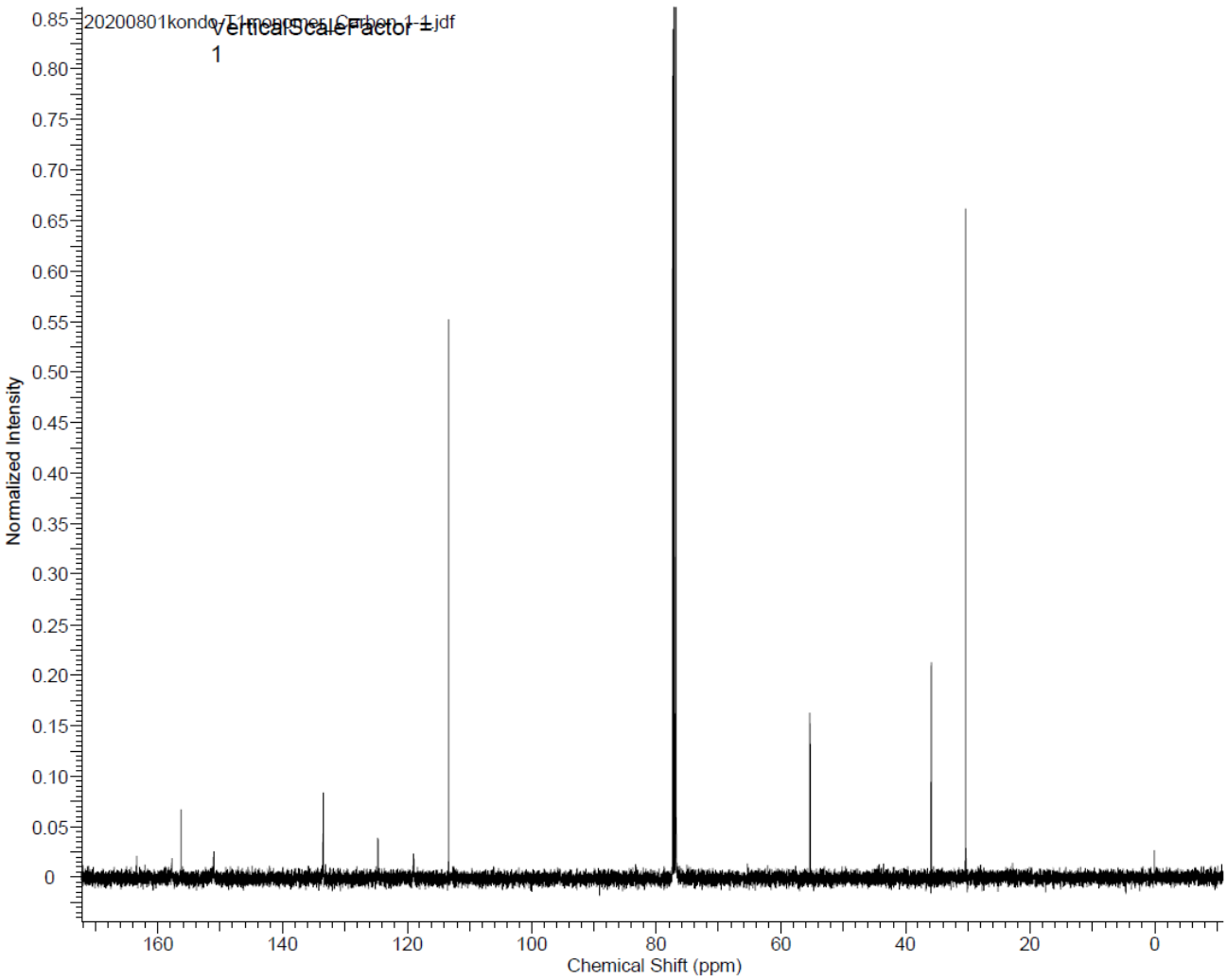

Fig. S4 ^{13}C NMR spectrum of **3** ($CDCl_3$, 125 MHz).

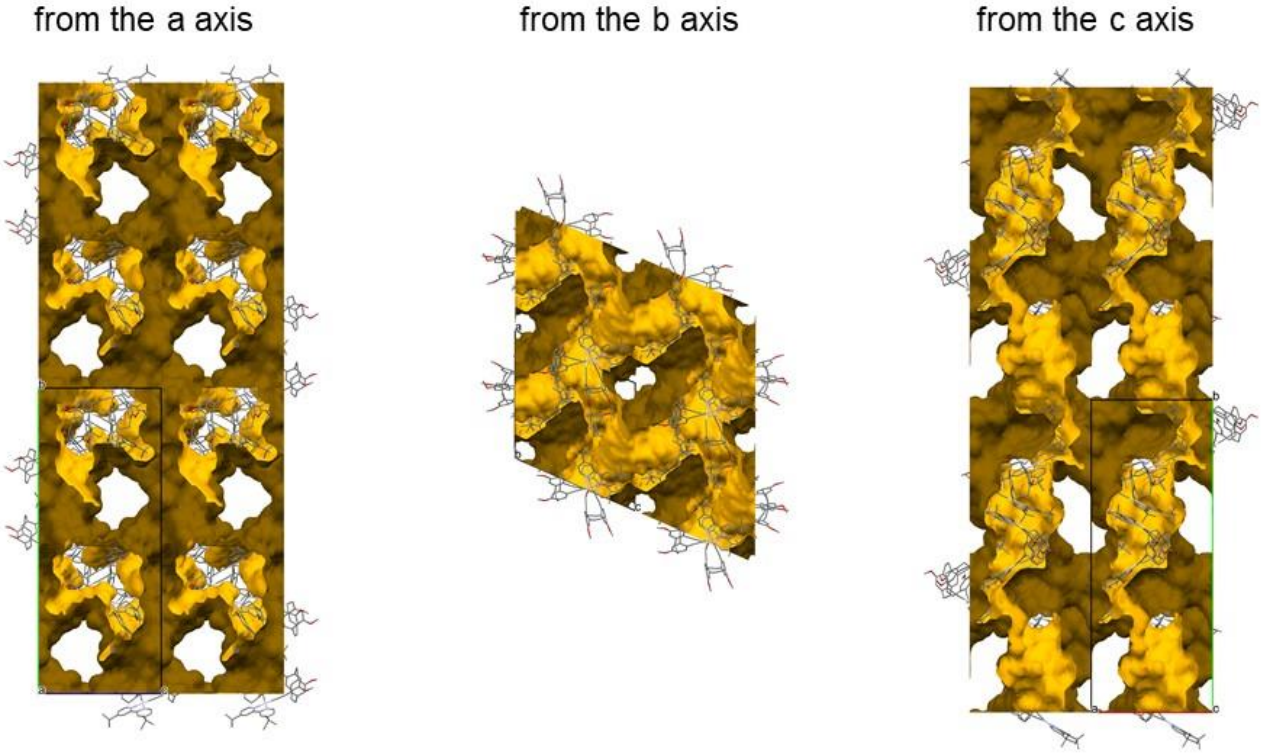

Fig. S5 Solvent accessible surface area of (R_p,R_p)-**2**.

Table S1 Crystallographic data and structure refinements for (R_p,R_p)-**2**.

Parameter	(R_p,R_p)-**2**
Formula	$C_{80}H_{86}N_4O_4Pt_2$
Formula weight	1557.70
Temperature (K)	123
Crystal color, habit	red, needle
Crystal size, mm	0.10 × 0.05 × 0.05
Crystal system	monoclinic
Space group	$P2_1$ (#4)
a, Å	21.7528(3)
b, Å	51.3282(5)
c, Å	22.4375(3)
α, deg	90
β, deg	113.3919(17)
γ, deg	90
V, Å^3	22993.1(6)
Z value	15
D_{calcd}, g cm^{-3}	1.687
μ (Mo$_{K\alpha}$), cm^{-1}	46.18
F(000)	11730.0
$2\theta_{max}$, deg	58.0
No. of reflections measured	218948
No. of observed reflections	105599
No. of variables	3242
R_1 (I > 2σ(I))[a]	0.0619
wR_2 (all reflns)[b]	0.1907
Goodness of fit	0.879

[a] $R_1 = \Sigma(|F_o|-|F_c|)/\Sigma(|F_o|)$. [b] $wR_2 = [\Sigma[w(F_o^2-F_c^2)^2]/\Sigma w(F_o^2)^2]^{1/2}$.

Table S2 Photophysical data for **2** and **3**.

Complex	$\lambda_{abs,max}$ [nm]		$\lambda_{lum,max}$ [nm][c]		Φ[c,d]		τ [μs][e]		$\lvert g_{abs}\rvert$:$\lvert g_{lum}\rvert$[f]	
	solution[a]	film[b]	solution[a]	film[b]	solution[a]	film[b]	solution[a]	film[b]	solution[a]	film[b]
2	432	399	656	610	0.001	0.007	N. D.	0.02, 0.07	0.001:0.001	0.001:0.001
3	431	-	601	-	0.025	-	0.10, 0.45	-	-	-

[a] Data were obtained from a 2.0×10^{-4} M solution in toluene at 298 K. [b] Data were obtained from a 10 wt% PMMA film at 298 K. [c] Excited at each $\lambda_{abs,max.}$ [d] Determined by the absolute method using an integrating sphere. [e] Excited at 340 nm. [f] Excited at 350 nm.

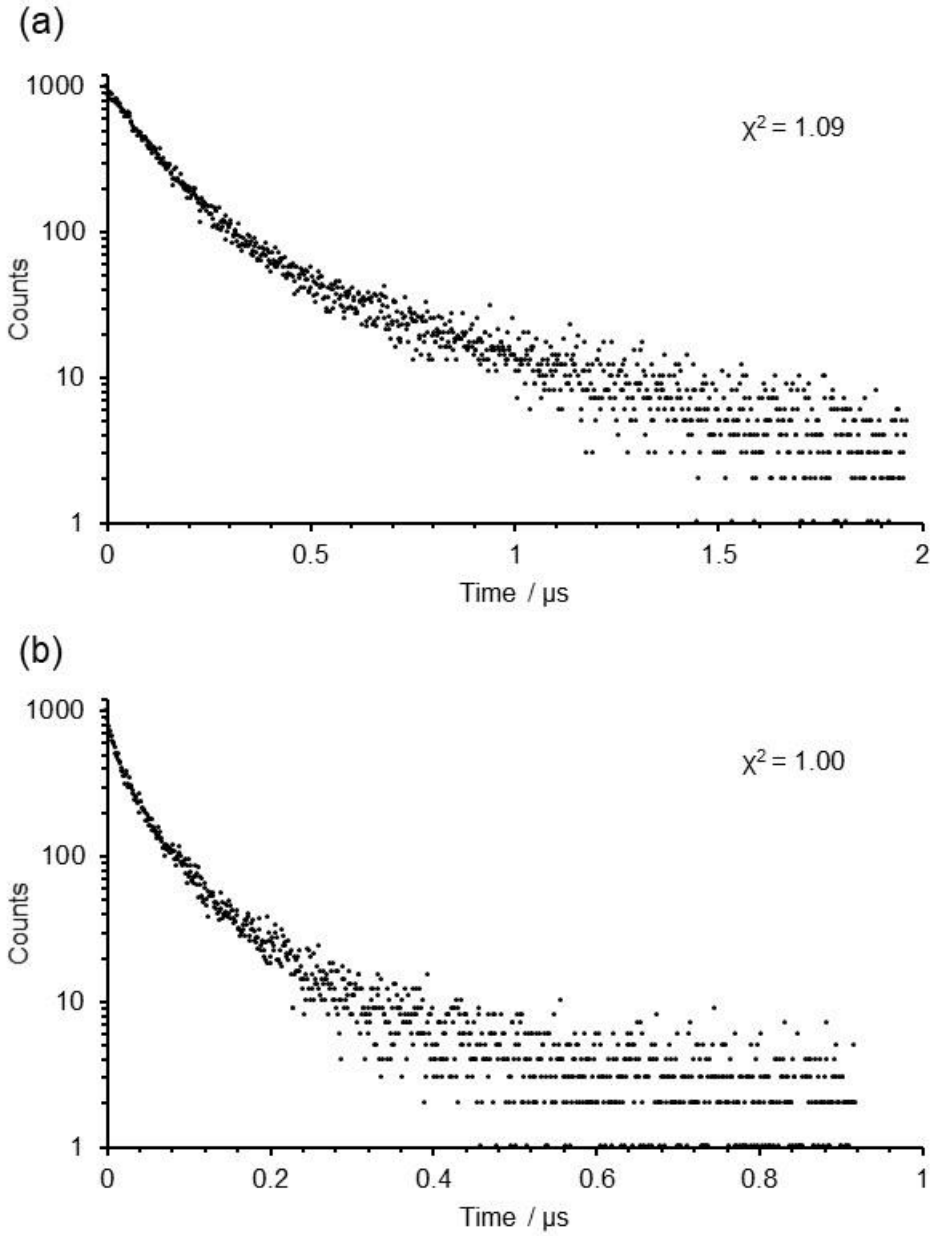

Fig. S6 Emission decay curves for (a) **3** in degassed toluene (2.0×10^{-4} M) and (b) (R_p,R_p)-**2** in PMMA film (10 wt%) monitored at each λ_{max} at 298 K (λ_{ex} = 340 nm).

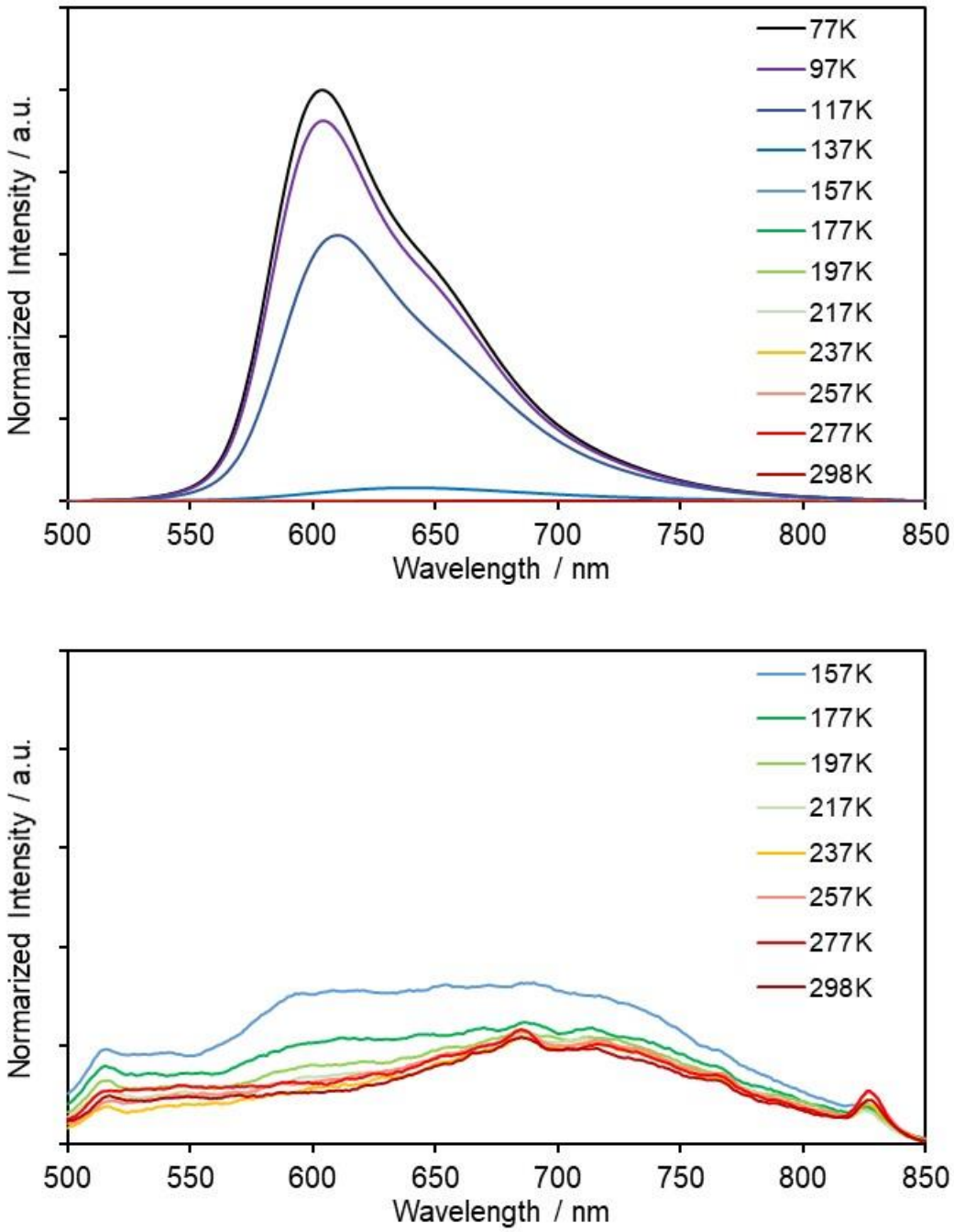

Fig. S7 Temperature-dependence of emission for (R_p,R_p)-**2** in 2-MeTHF (2.0×10^{-4} M) at 77–298 K (λ_{ex} = 502 nm).

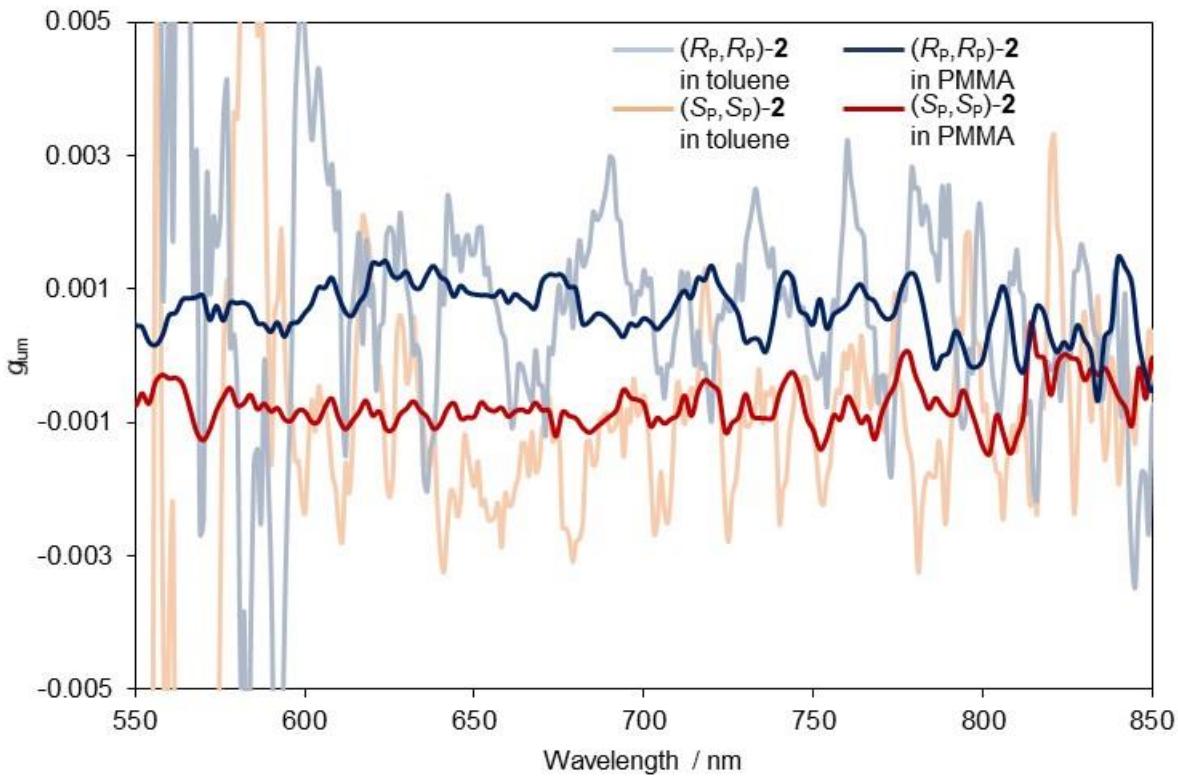

Fig. S8 Charts of g_{lum} of (R_p,R_p)- and (S_p,S_p)-**2** in toluene (2.0×10^{-4} M) and PMMA film (10 wt%).

<u>Determination of $|g_{lum}|$ values of (R_p,R_p)- and (S_p,S_p)-**2** in toluene (2.0×10^{-4} M) and PMMA film (10 wt%)</u>

Because of the low quantum efficiency of the emission from platinum complex at room temperature in both states, the CPL spectra must become noisy. Thus, we obtained the absolute dissymmetry factors $|g_{lum}|$ by equation (S1) and (S2).

(S1) $|g_{lum}| = (|g_{lum,R}|+|g_{lum,S}|)/2$

(S2) $|g_{lum,R}|$ and $|g_{lum,S}|$= absolute averaged value of the g_{lum} of each enantiomer in a wavelength of 657–757 nm (λ_{PLmax} ±50 nm) for toluene solution and 606–646 nm (λ_{PLmax} ±20 nm) for PMMA film

The λ_{PLmax} is the λ_{max} of corresponding non polarized emission recorded on a JASCO CPL-300.

Calculated values are shown below.

$|g_{lum,R}|$ in toluene = 0.73×10^{-3}

$|g_{lum,S}|$ in toluene = 1.27×10^{-3}

$|g_{lum}|$ in toluene = 1.0×10^{-3}

$|g_{lum,R}|$ in PMMA = 1.09×10^{-3}

$|g_{lum,S}|$ in PMMA = 0.88×10^{-3}

$|g_{lum}|$ in PMMA = 1.0×10^{-3}

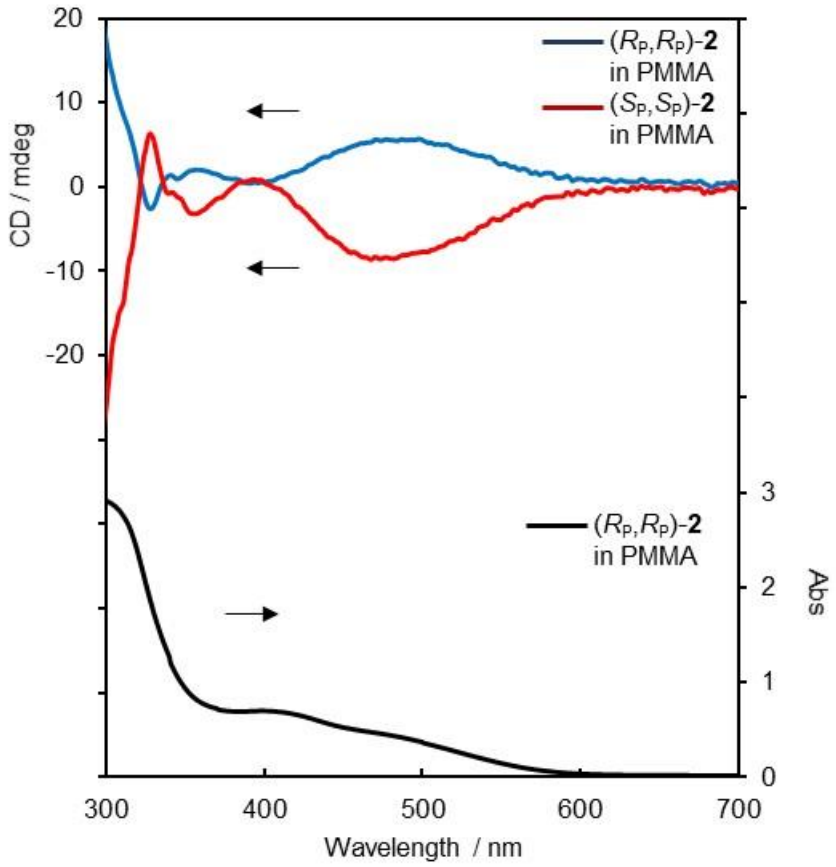

Fig. S9 UV/Vis absorption and CD spectra of (R_p,R_p)- and (S_p,S_p)-**2** in PMMA film (10 wt%).

Table S3 Selected data for singlet excitation energy, major configuration, coefficient, oscillator strength, and the character of charge transfer for (R_p,R_p)-**2**.[a]

State	Excitation energy / eV (/nm)	Major configuration	Coefficient	Oscillator strength	Character
S_1	2.76 (450)	H(a)→L(a)	0.35272	0.0818	[1]LLCT
		H(b)→L(b)	0.29265		
S_2	2.76 (450)	H(a)→L(b)	0.35606	0.1291	[1]LLCT
		H(b)→L(a)	0.29789		

[a]Estimated from TD-DFT calculations (LC-BLYP/ZORA-def2-SVP, SARC-ZORA-SVP with relativistic ZORA Hamiltonian) based on ground state optimized structure (MN15/6-31G(d), LanL2DZ). H: HOMO, L: LUMO.

Table S4 Transition electronic and magnetic dipole moments of singlet transitions for (R_p,R_p)-**2**.[a]

State	|TEDM| / a.u.			|TMDM|[b] / a.u.		
	x	y	z	x	y	z
S_1	-0.00011	-0.00005	-1.10104	-0.00004	0.00004	-0.26458
S_2	1.24217	0.60737	-0.0001	0.45350	-0.63244	-0.00002

[a]Estimated from TD-DFT calculations (LC-BLYP/ZORA-def2-SVP, SARC-ZORA-SVP with relativistic ZORA Hamiltonian) based on ground state optimized structure (MN15/6-31G(d), LanL2DZ). [b]The value outputted by Orca program is exactly half from true value due to the program error. TEDM: Transition electronic dipole moment, TMDM: Transition magnetic dipole moment.

Table S5 Selected data for SOC excitation energy, major configuration, coefficient, oscillator strength, and the character of charge transfer for (R_p,R_p)-**2**.[a]

State	Excitation energy / cm^{-1} (/nm)	Configuration	Weight	Oscillator strength	Character
SOC_1	16253.5 (615)	$T_{2,0}$	0.30269	0.000018839	^{3}LLCT
		$T_{1,1}$	0.29265		
		$T_{1,-1}$	0.29266		
SOC_2	16253.7 (615)	$T_{1,0}$	0.36816	0.000012515	^{3}LLCT
		$T_{2,1}$	0.26022		
		$T_{2,-1}$	0.26022		
SOC_3	16253.7 (614)	$T_{1,0}$	0.51801	0.000623664	^{3}LLCT
		$T_{2,1}$	0.18828		
		$T_{2,-1}$	0.18828		
SOC_4	16288.0 (614)	$T_{2,0}$	0.58775	0.000147529	^{3}LLCT
		$T_{1,1}$	0.1539		
		$T_{1,-1}$	0.1539		
SOC_5	16314.6 (613)	$T_{1,1}$	0.45084	0.000248374	^{3}LLCT
		$T_{1,-1}$	0.45084		
SOC_6	16317.1 (613)	$T_{2,1}$	0.44892	0.000205480	^{3}LLCT
		$T_{2,-1}$	0.44892		
SOC_7	18390.4 (544)	S_1	0.56827	0.067287054	^{1}LLCT
		$T_{3,-1}$	0.11615		
		$T_{3,1}$	0.11615		
SOC_8	18413.9 (543)	S_2	0.55511	0.044409541	^{1}LLCT
		$T_{4,-1}$	0.12486		
		$T_{4,1}$	0.12486		

[a]Estimated from SOC-TD-DFT calculations (LC-BLYP/ZORA-def2-SVP, SARC-ZORA-SVP with relativistic ZORA Hamiltonian) based on ground state optimized structure (MN15/6-31G(d), LanL2DZ). H: HOMO, L: LUMO.

Table S6 Absolute TEDM and TMDM of SOC_1–SOC_6 for (R_p,R_p)-**2**.[a]

State	|TEDM| / a.u.			|TMDM|[b] / a.u.			
	x	y	z	x	y	z	$\|\cos\theta\|$
SOC_1	0.00097	0.00052	0.01950	0.00046	0.00598	0.02706	0.968
SOC_2	0.01398	0.00750	0.00133	0.00658	0.08586	0.00190	0.535
SOC_3	0.10970	0.02411	0.00006	0.02100	0.02822	0.00004	0.755
SOC_4	0.00008	0.00004	0.05461	0.00002	0.00002	0.04982	1.000
SOC_5	0.00087	0.00063	0.07079	0.00048	0.00024	0.05522	1.000
SOC_6	0.05374	0.03544	0.00146	0.02614	0.01526	0.00114	0.997

[a]Estimated from SOC-TD-DFT calculation (LC-BLYP/ZORA-def2-SVP, SARC-ZORA-SVP with relativistic ZORA Hamiltonian) based on optimized structure of lowest triplet state (UMN15/6-31G(d), LanL2DZ). [b]The value outputted by Orca program is exactly half from true value due to the program error. TEDM: Transition electronic dipole moment, TMDM: Transition magnetic dipole moment.